



City Research Online

City, University of London Institutional Repository

Citation: Sun, Z., Schrijer, F. F. J., Scarano, F. & van Oudheusden, B. W. (2012). PIV investigation of the 3D instantaneous flow organization behind a micro-ramp in a supersonic boundary layer. Paper presented at the 28th International Symposium on Shock Waves, 17-07-2011 - 22-07-2011, Manchester, UK. doi: 10.1007/978-3-642-25685-1_63

This is the accepted version of the paper.

This version of the publication may differ from the final published version.

Permanent repository link: <https://openaccess.city.ac.uk/id/eprint/7375/>

Link to published version: https://doi.org/10.1007/978-3-642-25685-1_63

Copyright: City Research Online aims to make research outputs of City, University of London available to a wider audience. Copyright and Moral Rights remain with the author(s) and/or copyright holders. URLs from City Research Online may be freely distributed and linked to.

Reuse: Copies of full items can be used for personal research or study, educational, or not-for-profit purposes without prior permission or charge. Provided that the authors, title and full bibliographic details are credited, a hyperlink and/or URL is given for the original metadata page and the content is not changed in any way.

City Research Online:

<http://openaccess.city.ac.uk/>

publications@city.ac.uk

PIV Investigation of the 3D Unsteady Flow Organization behind a Micro-Ramp in a Supersonic Boundary Layer

Z. Sun, F. J. J. Schrijer, F. Scarano, B. W. van Oudheusden

Summary. The flow field resulting from a single micro-ramp in a $Ma=2.0$ supersonic boundary layer is investigated using tomographic particle image velocimetry (Tomo-PIV). The measurements were carried out within two volumes behind the micro-ramp. Mean flow characteristics are analyzed, evidence of the streamwise vortex pair is given. In the instantaneous flow, a Kelvin-Helmholtz (K-H) instability developing in the wake of the element is revealed, and the K-H vortices are further identified. A conceptual model is provided to describe the instantaneous flow organization generated by a single micro-ramp.

1. Introduction

Shock wave boundary layer interaction (SWBLI) is a critical flow phenomenon involved in many high speed aerodynamic applications, such as supersonic inlets and external surfaces. Much effort has already been inserted to investigate the mechanism of SWBLI and its turbulent and unsteady nature. Meanwhile different types of flow control techniques are developed with the aim of diminishing those adverse effects introduced by SWBLI, such as flow separation and fluctuating pressure load. Micro-ramp vortex generator has been so far a popular and beneficial type of passive boundary layer control technique, it introduces less drag compared to conventional larger vortex generators while is still able to maintain the effectiveness of reducing flow separation.

Initiated by Anderson \cite{2470_Anderson}, who performed an optimization research on the geometric parameters of micro-ramps (angle of incidence, height, chord length) and delivered an optimal suggestion, investigations towards the working principles have been performed both experimentally and numerically. A mean flow description featured by Babinsky \cite{2470_Babinsky} depicts the streamwise counter rotating vortex pair and several accompanying secondary vortices in streamwise direction. The general working mechanism of the micro-ramp can be proposed through this mean flow description: the boundary layer is energized by the high momentum fluid in the free stream entrained by the downwash effects of the streamwise primary vortex pair. This results in a fuller boundary layer which it is more capable of enduring the adverse pressure gradient introduced by incident shock waves. However, due to the strong three-dimensional effects of the flow past a micro-ramp, the instantaneous flow structure is rather perplexing. Discussion on the instantaneous pattern is going on. Blinde et al.\cite{2470_Blinde} identified several vortex pairs developing downstream of the micro-ramp array visualized by stereo-PIV on two planes parallel to the flow floor at different heights. These vortex pairs were recognized as the cross sections of legs of hairpin vortices similar to the hairpins that appeared in a turbulent boundary layer. A conceptual model of a train of hairpin vortices developing downstream of a micro-ramp was formulated. An LES simulation of the flow past a single micro-ramp performed by Li \cite{2470_Li01} visualized a series of vortex rings behind the trailing edge. This ring structure was referred to as a new mechanism in micro-ramp flow control. A recent experimental research performed by Lu \cite{2470_Lu} using laser sheet visualization revealed pronounced Kelvin-Helmholtz structures with large intermittency developing downstream of micro-ramps. According to the explanation by Lu, the KH instability structures developed from the streamwise primary vortices, which were more stable when close to the micro-ramp and broke down to form larger roller structures with large intermittency when traveling further downstream. Since the large intermittent pattern emerges as a new research focus, it is demanding to define this structure.

Inspired by the foregoing efforts, present experimental study using tomo-PIV was carried out with the aim of revealing the instantaneous flow organization behind a single micro-ramp inside a supersonic boundary layer.

2. Experimental Arrangement

Experiments were carried out in the blow-down supersonic wind tunnel (ST15) of High Speed Aerodynamics Laboratory at Delft University of Technology. In the present study, the wind tunnel was operated at Mach 2.0 (free stream velocity $U_\infty=532$ m/s), with a stagnation pressure of $P_0=3.2$ bar. The boundary layer along the tunnel floor was selected for the micro-ramp investigation. After developing approximately 0.5 m past the throat section of the nozzle, the boundary layer obtained a thickness of 4.8 mm.

The investigated micro-ramp height is 4 mm, the other dimensions are scaled to the height according to the recommendation from Anderson [2470_Anderson] resulting in a chord length of 27.4 mm and a spanwise width of 24.4 mm.

Tomo-PIV, which is most recent extension of PIV, was used as measurement technique, and measurements were carried out within two volumes 35 mm downstream of the micro-ramp. These two volumes are of identical size, which is $25 \times 15 \times 6$ mm³. The layout of the experimental setup is shown in Figure 1.

The flow was seeded by DEHS with the nominal diameter of approximately 1 μm . Particles were ejected into the flow through a seeding tube upstream of the settling chamber. The seeded flow was illuminated by a Spectra-Physics Quanta Ray PIV-400 double pulse Nd:Yag laser at a wavelength of 532 nm. Each pulse has energy of 400 mJ and duration of 6 ns. A laser probe was inserted from the side wall downstream of the test section, through which the laser beam was shaped into volume.

Three PCO Sencicam QE CCD cameras with the sensor of 1376 X 1040 pixels were installed and equipped with Nikon 105 mm objectives respectively. Images were recorded at a rate of 5 Hz and the separation between each consecutive exposure was 0.6 μs . As a result, a digital image resolution of 43.7 pixel/mm was achieved and the free stream vector obtained a length of 14 pixels. 400 images were recorded for each volume so that data convergence is guaranteed.

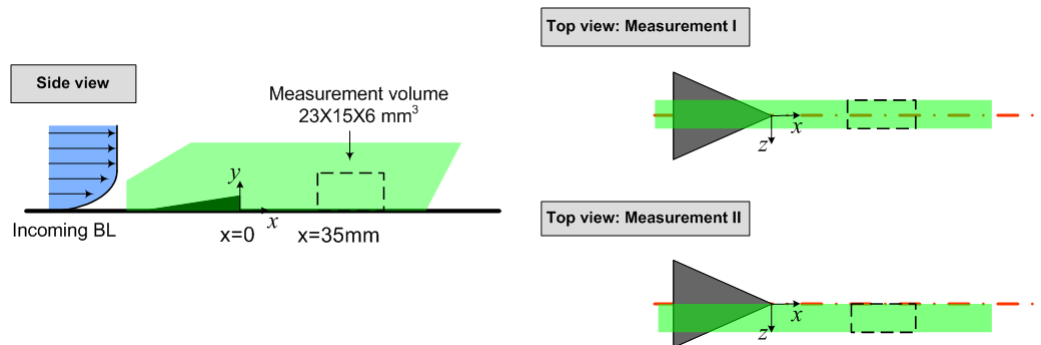


Figure 1. Experimental layout of the micro-ramp and laser illuminations.

3. Results and Analysis

3.1 Mean Flow Characteristics

Previous studies on the micro-ramp indicate the streamwise counter rotating vortices, which are symmetrical to the center plane ($z=0$), are the dominating structure in the mean flowfield. Four planes at different streamwise locations are selected to represent the mean flow organization and shown in figure 2. It should be noted that the results are from Measurement II and are mirrored across the center plane ($z=0$), through which the flow are assumed symmetrical. It is straightforward to observe the contour rotating vortices through the vectors overlaid on the contour plots. The upwash (red in color in v -component contours) and downwash (blue in color in the same contours) visualized through v -component also provide proof for the streamwise vortices. These two vortices are close to each other in upstream locations, and they depart and are lifted while travelling downstream.

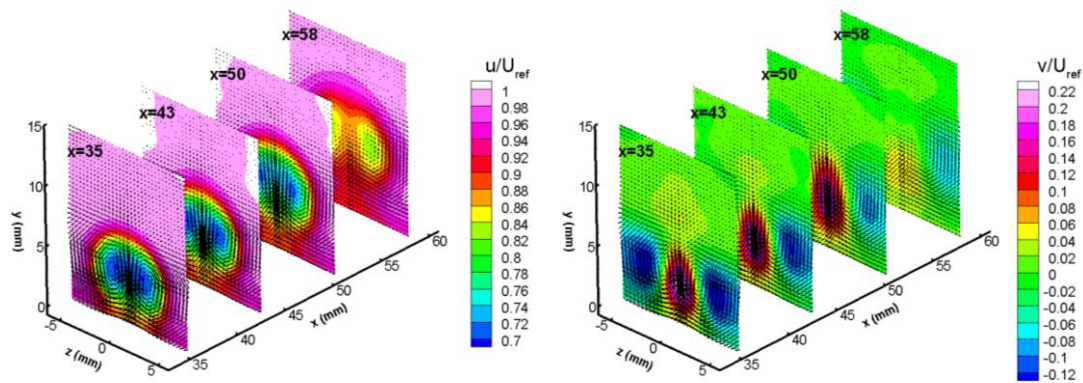


Figure 2. Selected contour planes of the mean flow field, left: u -component, right: v -component.

A wake region which includes the streamwise vortex pair can be observed from the u -component contours. It displays a circular shape and maintains to downstream locations. It also expands and is lifted along its development. A shear layer of u -component locates at the outer edge of the wake, which reduces the streamwise velocity from $1.0U_\infty$ to approximately $0.8U_\infty$.

3.2 Turbulent Characteristics

Turbulent properties are responsible for the instantaneous flow structures. As a result they are discussed in this section. The distributions of both fluctuation components, namely $\langle u' \rangle$ and $\langle v' \rangle$, at the center plane ($z=0$) shown in figure 3 reveal their similar shear layer structures with higher fluctuations at center and lower fluctuations at both edges.

Detailed profiles of both components at $x=40$ mm are shown in figure 4. The streamwise velocity profile is also included for positioning the shear layers, but the scale of horizontal axis could not be applied. From the velocity profile, the wake is comprised of the upper and lower shear layers. According to figure 4, within both shear layers, $\langle u' \rangle$ and $\langle v' \rangle$ exhibit considerable increase and the maximums are reached in the upper shear layer. Although the positions of maximum fluctuation components are different, they are rather close with a distance of approximately 1 mm. If attention is paid to the magnitude of each fluctuation component, $\langle v' \rangle_{\max}$ is larger than $\langle u' \rangle$, which suggests the anisotropy of this flow.

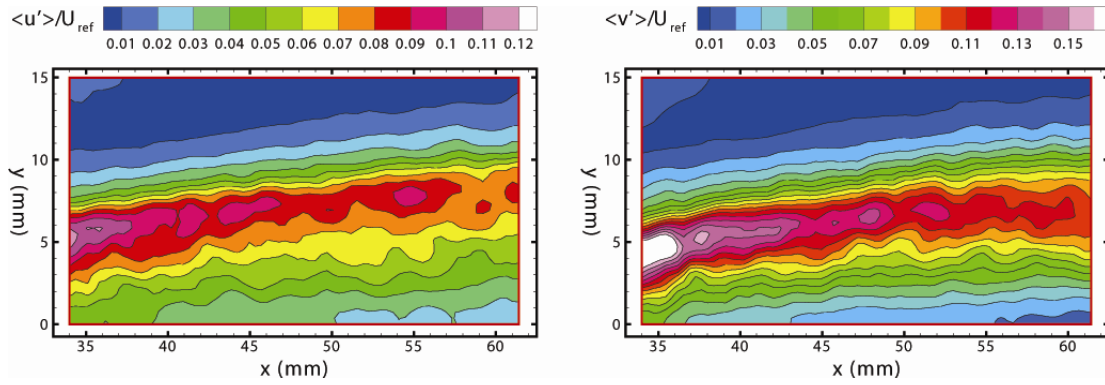


Figure 3. Fluctuation velocity distributions at the center plane ($z=0$), left: $\langle u' \rangle$, right: $\langle v' \rangle$

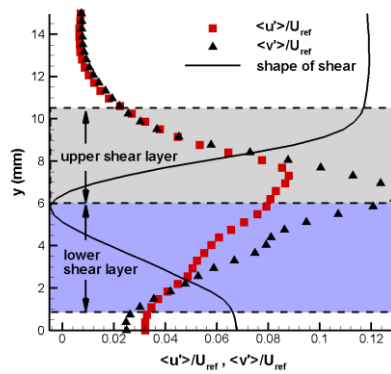


Figure 4. Profile of velocity fluctuation at $x=40 \text{ mm}$ in the center plane.

3.3 Cross-Sectional Representations

Although three-dimensional flowfield can be achieved through Tomo-PIV measurement, cross-sectional contour plots still obtain the strength in representing the flow. As a result, two cross-sectional contours of u -component, one in y - z plane at $x=42 \text{ mm}$ and the other in x - y plane at $z=0$, are extracted from the same three dimensional flowfield and shown in figure 5.

The dominating streamwise vortex pair is revealed in the y - z plane; however its appearance, which is not symmetrical to the center plane, is different from that in the mean flow. Due to the instantaneous property, a meandering behavior is expected for the vortices. The shape of the wake exhibits a unsmooth edge, which is a smooth and circular in the mean flow.

A classical Kelvin-Helmholtz instability characterized by the wavy interface is visualized in the x - y plane. The KH instability occurs in a velocity shear with sufficient difference. After subtracting a constant value in the vector field, the KH vortices are visualized, which are indicated by circles in contour. These K-H vortices have a clockwise rotational direction; as a result local accelerations and decelerations are introduced on the upper and lower sides of the vortices, respectively. Because of the upside acceleration three dimples with high streamwise velocity are produced in this visualization, accordingly the core of the wake is separated by a few low speed regions due to the lower side deceleration. It should be noted that the strip with high streamwise velocity on top of the wake in the y - z contour is a cross section of the three dimensional KH instability induced high speed region.

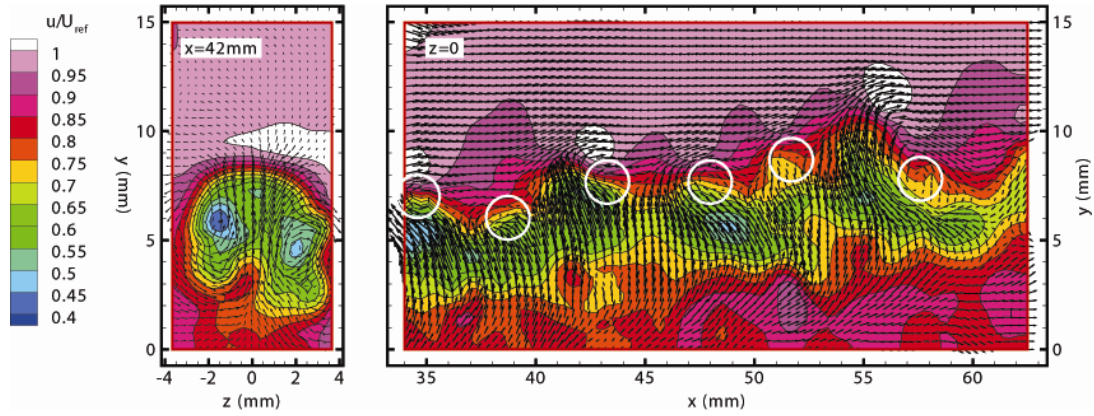


Figure 5. Cross-sectional contour of u-component, left: y-z plane, right: x-y plane (a constant value has been subtracted from the original vectors)

3.4 Volumetric Representation

The main results of this study are presented in this section. Velocity and vorticity isosurfaces are used to further characterize the flow. It should be noted that the flowfield shown in figure 6 has the same origin as the cross-sectional flowfields in figure 5. Two values of u-component are displayed: high speed in pink ($1.02U_\infty$) and low speed in green ($0.8U_\infty$), which correspond to the KH vortices induced high and low speed regions explained through cross-sectional observation. Both regions are separate in space and exhibit similar intermittency as KH instability.

Vorticity structures are also displayed. Both categories of vortices, namely the streamwise and KH vortices are visualized. The streamwise vortices are presented through ω_x in different colors, because of their opposite rotational directions. The intermittent KH vortices are presented through ω_z . Although only the top part of the KH vortices are visualized, an arc shape can be expected for the KH vortices which follow the shape of the instantaneous shear layer in y-z plane.

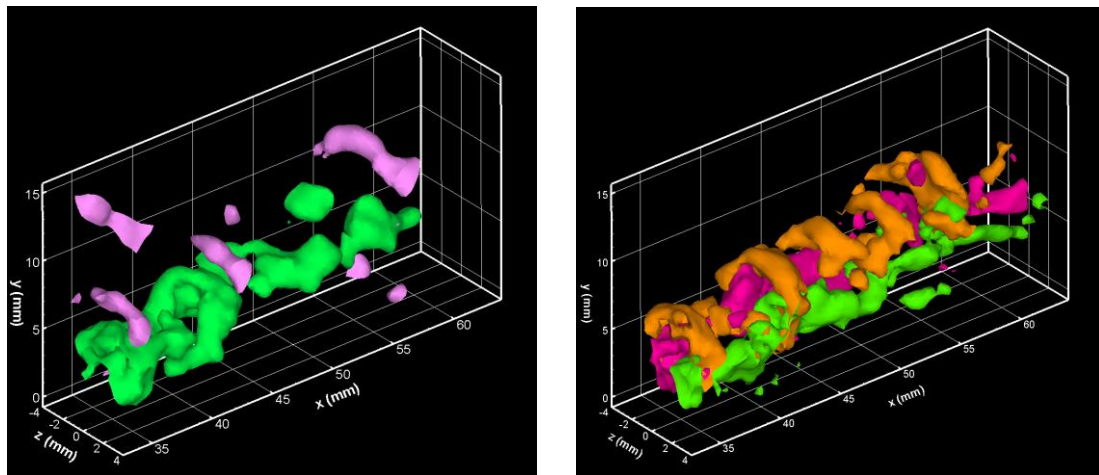


Figure 6. Volumetric representation, left: isosurfaces of u-component, right: isosurfaces of vorticity.

4. A Conceptual Model and Conclusions

According to the analysis and discussions above, two categories of vortices are developing in the instantaneous flow generated by a micro-ramp: the streamwise counter rotating vortices and the arc-shaped KH vortices. An illustration describing this instantaneous flow is depicted in figure 7.

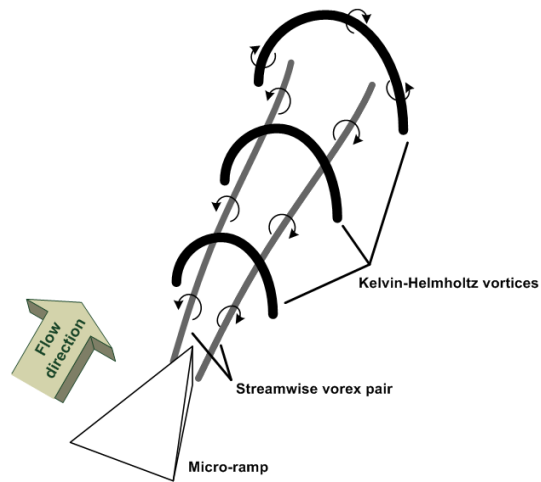


Figure 7. A conceptual model of the instantaneous vorticity structure.

As an end of this Tomo-PIV investigation of this particular flow, a few conclusions can be drawn. Firstly, Tomo-PIV is well suited for the measurement of this three-dimensional flow. Secondly, a new two-vortex structure can be built to describe the instantaneous flow, which is, as a matter of fact, compatible to the hairpin or vortex-ring descriptions.